Quantum Tricriticality at the Superfluid-Insulator Transition of Binary Bose Mixtures

Yasuyuki Kato,[1] Daisuke Yamamoto,[2] and Ippei Danshita[3,4]

[1]*RIKEN Center for Emergent Matter Science (CEMS), Wako, Saitama 351-0198, Japan*
[2]*Condensed Matter Theory Laboratory, RIKEN, Wako, Saitama 351-0198, Japan*
[3]*Yukawa Institute for Theoretical Physics, Kyoto University, Kyoto 606-8502, Japan*
[4]*Computational Condensed Matter Physics Laboratory, RIKEN, Wako, Saitama 351-0198, Japan*

Quantum criticality near a tricritical point is studied in the two-component Bose-Hubbard model on square lattices. The existence of a quantum tricritical point on a boundary of a superfluid-insulator transition is confirmed by quantum Monte Carlo simulations. Moreover, we analytically derive the quantum tricritical behaviors on the basis of an effective field theory. We find two significant features of the quantum tricriticality that are its characteristic chemical potential dependence of the superfluid transition temperature and a strong density fluctuation. We suggest that these features are directly observable in existing experimental setups of Bose-Bose mixtures in optical lattices.

Rapid development in experiments with ultracold gases confined in optical lattices has advanced the studies of quantum phase transitions (QPTs), thanks to their precise controllability of various parameters, such as external potentials, interparticle interactions, and lattice geometry, over a wide range. Several QPTs that are of close relevance to other condensed matter systems have been realized in experiments, such as superfluid (SF)-Mott insulator (MI) transitions in a variety of lattice geometries [1–4], SF-Bose glass transitions in a random [5,6] or quasiperiodic [7,8] potential, magnetic transitions in a tilted [9] or triangular [10,11] optical lattice, and topological transitions in a double-well optical lattice [12]. Recent experiments have reported even the observation of quantum critical behaviors accompanying the second-order QPT between vacuum and a SF [13], thus providing new opportunities for studying quantum criticality in optical-lattice systems.

Tricriticality, or, more generally, multicriticality, is a fundamental concept in the study of phase transitions [14]. A tricritical point (TCP) marks a point at which a second-order (continuous) phase transition changes to a first-order (discontinuous) phase transition on a single phase boundary in a two parameter phase diagram. Tricriticality has been discussed in the contexts of several condensed matter systems, e.g., $FeCl_2$ [15], ^3He-^4He mixtures [16], and correlated electron materials [17,18], as well as in quantum chromodynamics [19]. Due to its unique nature, unconventional critical properties are expected to—and indeed are found to—emerge in the vicinity of a TCP. As such, exploration of TCPs can be a useful strategy for finding novel universality classes of phase transitions. Despite such ubiquity and importance of TCPs, understanding of quantum tricriticality remains limited to a phenomenological level because of lack of experiments with flexible controllability and exact numerical simulations on a microscopic model, in contrast to the classical one.

In this Letter, we use the unbiased numerical method of quantum Monte-Carlo (QMC) simulations based on the Feynmann path integral [20] to show the existence of quantum TCPs in the ground state phase diagram of the two-component Bose-Hubbard model (BHM) on square lattices. This result suggests that quantum tricriticality can realistically be studied in Bose-Bose mixtures trapped in optical lattices, which are subsistent experimental setups [21–26]. From a simple mean-field (MF) analysis, we explain that effective two-body attraction causes the emergence of the TCPs. Furthermore, analyzing an effective continuum model, we derive critical behaviors regarding the TCP. In the finite-temperature phase diagrams obtained by the QMC method, we identify the quantum tricritical behavior of the SF-normal transition temperature, which can be directly measured in experiments [13].

We consider the two-component BHM on square lattices ($d = 2$) [27]

$$\mathcal{H} = -t \sum_{\alpha,\langle j,l \rangle} (b_{\alpha,j}^\dagger b_{\alpha,l} + \text{H.c.}) - \mu \sum_{\alpha,j} b_{\alpha,j}^\dagger b_{\alpha,j}$$
$$+ \sum_{\alpha,\alpha',j} \frac{U_{\alpha\alpha'}}{2} b_{\alpha,j}^\dagger b_{\alpha',j}^\dagger b_{\alpha',j} b_{\alpha,j}, \qquad (1)$$

where $b_{\alpha,j}^\dagger$ ($b_{\alpha,j}$) is a creator (annihilator) of an α-type boson at site j, t is the nearest neighbor hopping amplitude, μ is the chemical potential, and $U_{AA} = U_{BB} \equiv U > 0$ ($U_{AB} = U_{BA}$) is the on-site intracomponent (intercomponent) repulsive interaction. This model describes Bose-Bose mixtures confined in an optical lattice [21–26]. In the optical-lattice experiments, U/t is controlled by changing the depth of the optical lattices [27], and U_{AB} is controlled by using Feshbach resonances [23,28,29] or component-dependent optical lattices [26,30]. Although the hopping amplitudes are different for each component, in general, we

use a common value t for simplicity. Indeed, in a gas of ^{87}Rb having two atomic spin states as an internal degree of freedom, the difference of hopping amplitudes between these two spin states is negligible [22]. Notice that we choose $\hbar = k_B = a = 1$ as our units throughout the Letter, where a is the lattice constant.

When $d \geq 2$, the possibility of the first-order QPT from the SF to the MI phase with even fillings has been previously suggested by Monte Carlo simulations on the two-component J-current model [31], which is a $(d+1)$-dimensional classical analog of Eq. (1), and MF analyses on Eq. (1) [32,33]. Similar first-order QPTs have been found also in other related models [34,35]. Below, we demonstrate the presence of the first-order QPT and the associated TCPs in the $t-\mu$ phase diagram by means of direct QMC simulations on Eq. (1).

We apply the worldline QMC method to the model (1) with a periodic boundary condition. We use a modified version [36] of the directed-loop algorithm [37] for updating worldline configurations. Although the modification is originally made for the single component BHM, it is also crucial for this application. We set the maximum occupation number at a single site as $n_{\text{max}} = 4$ for each component.

Figure 1 shows the ground-state phase diagram of the model (1) near the $n = 2$ Mott lobe at $U_{AB}/U = 0.9$, where $n \equiv n_A + n_B$ is the total density and n_α is the density of type-α bosons. At this value of U_{AB}/U, the phase separation does not occur in either the SF or MI phase. The phase boundary of the second-order QPT between the SF and MI phase is determined from the single-particle and single-hole Mott gaps estimated by using the QMC data of
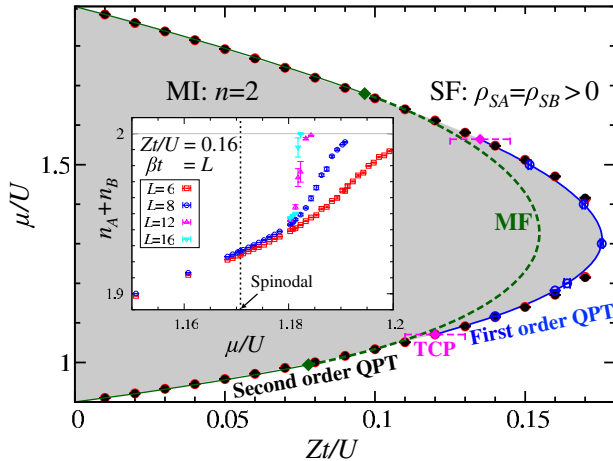
FIG. 1 (color online). Ground state phase diagram at $U_{AB}/U = 0.9$ computed with QMC and MF methods. Thick (thin) green solid line shows the phase boundary of the first (second)-order QPT computed by MF analysis. Black (red) closed circles are the second-order QPT points or spinodals computed by QMC simulations at $L = 16$ ($L = 12$) and $\mu/U = 1.35$. Blue open circles are the first-order QPT points at $L = 16$. Diamonds are TCPs. Inset: μ dependence of total density of bosons at $Zt/U = 0.16$.

the Green's function $\langle b_{A,\boldsymbol{k}}(\tau) b_{A,\boldsymbol{k}}^\dagger(0) \rangle$ at $\boldsymbol{k} = 0$ [38], where $b_{A,\boldsymbol{k}}^\dagger \equiv L^{-d/2} \sum_j b_{A,j}^\dagger \exp(i\boldsymbol{k} \cdot \boldsymbol{x}_j)$ and $\boldsymbol{x}_j$ represents the position vector of site j. We estimate the Mott gaps at $\mu/U = 1.35$ and $L = 12$ and 16 with several values of Zt/U. In the scale of the phase diagram (Fig. 1), finite-size effects are negligible. In the case of the first-order QPT, the Mott gaps do not locate the phase boundary, but the spinodal of the MI state. To identify the first-order phase boundary, we calculate the total density n near the tip of the $n = 2$ Mott lobe as a function of μ/U or Zt/U as shown in the inset of Fig. 1. At $Zt/U = 0.16$, we find a clear jump in n versus μ/U, and we determine the transition point from the position of the jump for $L = 16$. The spinodal located by the Mott gap is well separated from the true transition point and is located in the SF side. When Zt/U decreases, the jump becomes smaller and is supposed to vanish at the TCP. However, it is practically very difficult to estimate numerically the position of the TCPs from the vanishment of the jump, because the jump is too small to be detected close to the TCPs.

Instead, we determine the TCPs from the difference in the critical behavior of the density fluctuation $\kappa \equiv \partial n / \partial \mu$ between the generic [39] and tricritical transitions. Since the density of atoms is locally observable in optical-lattice experiments [40], this density fluctuation can be directly probed. To determine the critical behavior across the transition between the MI phase with even filling and the SF phase with incommensurate filling, we analyze the effective action in continuum given by

$$
\begin{aligned}
S^{\text{eff}} = \beta V f_0 + \int d\tau \int d^d x \Bigg[&\sum_\alpha \left(\psi_\alpha^* \frac{\partial \psi_\alpha}{\partial \tau} + \frac{1}{2m} |\nabla \psi_\alpha|^2 \right. \\
&\left. - r_\alpha |\psi_\alpha|^2 + \frac{u}{2} |\psi_\alpha|^4 + \frac{w}{3} |\psi_\alpha|^6 \right) + u_{AB} |\psi_A|^2 |\psi_B|^2 \\
&+ w_{AB} (|\psi_A|^4 |\psi_B|^2 + |\psi_A|^2 |\psi_B|^4) \Bigg],
\end{aligned} \tag{2}
$$

where $\beta \equiv T^{-1}$ is the inverse temperature, $V \equiv L^d$ is the volume, and f_0 is the free energy density of the MI state. A derivation of the effective model is shown in detail in the Supplemental Material [41]. In Eq. (2), $\psi_\alpha(\boldsymbol{x}, \tau)$ denotes the SF order-parameter field of type-α bosons. Inclusion of terms up to the sixth order of ψ_α is necessary to describe the shift from the generic transition to the first-order one through the TCP. The dynamical and critical exponents for the transitions described by the action (2) are $z = 2$ and $\nu = 1/2$. Applying the MF theory combined with renormalization group analysis to the effective model (2), we obtain the critical behaviors of the density versus the chemical potential as shown in Table I. The results imply that in two dimension $\kappa \propto \ln(1/\delta\mu)$ for the generic transition while $\kappa \propto \delta\mu^{-1/2}$ for the tricritical one (see the Supplemental Material [41] for a detailed derivation). Here $\delta\mu \equiv |\mu - \mu_c|$ and μ_c denotes μ at the critical point.

TABLE I. Quantum criticality of the density $\delta n \equiv |n - n_0|$ measured on that at the MI state n_0 and the transition temperature T_c as functions of the chemical potential measured on the critical point $\delta\mu \equiv |\mu - \mu_c|$.

	Density	Transition temperature
$d = 2$ Generic	$\delta\mu \ln(1/\delta\mu)$	$\delta\mu \ln(1/\delta\mu)/\ln\ln(1/\delta\mu)$
$d = 2$ Tricritical	$\delta\mu^{1/2}$	$\delta\mu^{1/2}/\ln(1/\delta\mu)$
$d > 2$ Generic	$\delta\mu$	$\delta\mu^{2/d}$
$d > 2$ Tricritical	$\delta\mu^{1/2}$	$\delta\mu^{1/d}$

It is remarkable that for the tricritical case there is no logarithmic correction even in $d = 2$, which is the upper critical dimension. Utilizing these critical behaviors, the TCPs are determined as follows. In Fig. 2, we depict κ along the lower and upper edges of the lobe estimated by the Mott gap at $\mu/U = 1.35$ and $L = 16$. There we see that κ has a distinct peak at a certain value of Zt/U. The peak position identifies the TCPs at which κ diverges more strongly than at the generic QCPs or at the spinodal of the MI state. Notice that although κ diverges weakly as $\sim \ln(1/\delta\mu)$ even at generic QCPs in $d = 2$, the QMC data do not show such a divergence because the phase boundary computed with $L = 16$ is expected to be located inside the SF phase in the thermodynamic limit.

We discuss a physical mechanism for the shift of the QPT from second order to first order and the associated emergence of the TCP within a MF approximation. By the green line in Fig. 1, we show the phase boundary computed with the use of the MF theory [32,33] for comparison. While a quantitative difference in the first-order phase boundary and the TCP between the MF and QMC methods is discernible, the MF analysis correctly captures the qualitative features of the phase diagram. Applying the MF approximation $\psi_\alpha(\mathbf{x}, \tau) = \phi_\alpha$ to the effective model (2), we obtain the MF action $S^{\mathrm{mf}} = \beta V f$ with the free energy density written as

$$f = f_0 - 2r\phi^2 + (u + u_{AB})\phi^4 + \frac{2}{3}(w + 3w_{AB})\phi^6, \quad (3)$$

where $r_A = r_B \equiv r$. Taking into account the symmetry between the two components, we here set $|\phi_A| = |\phi_B| \equiv \phi$ that corresponds to the superfluid order parameter $\langle b_{\alpha,j} \rangle$ characterizing the SF-MI transition. From Eq. (3), one sees that the transition is of first order when $u + u_{AB} < 0$ while it is of second order when $u + u_{AB} \geq 0$. In Fig. 3, we plot $-u$ and u_{AB} as functions of Zt/U along the lower and upper edges of the lobe (see the Supplemental Material [41] for how to calculate u and u_{AB}). When Zt/U increases in the region $Zt/U > 0.05$, u_{AB} becomes strongly attractive so that $u + u_{AB}$ changes its sign at a certain point, which is nothing but the TCP. Thus, the shift of the QPT from second order to first order can be attributed to the strong intercomponent attraction, which leads to the collapse of the SF state at low SF density.
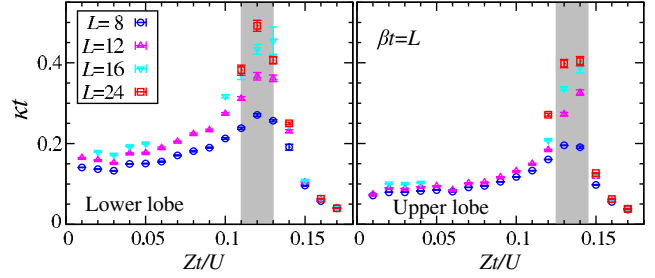
FIG. 2 (color online). Density fluctuation $\kappa \equiv \partial n/\partial\mu$ at the lower (left panel) and upper (right panel) edges of the lobe estimated from the particle and hole gaps. The shaded regions mark the peaks of κ.

To complete the ground-state phase diagram, one needs to reveal whether there exists the supercounterflow order in the MI phase [31]. In Fig. 4, we show the SF stiffness computed with QMC simulations from the fluctuation of winding numbers [42,43] as $\rho_{S\alpha} \equiv \langle W_\alpha^2 \rangle/(4\beta t)$, $\rho_{SC} \equiv \langle (W_A - W_B)^2 \rangle/(4\beta t)$, and $\rho_{SP} \equiv \langle (W_A + W_B)^2 \rangle/(4\beta t)$, where $W_\alpha^{x(y)}$ is a winding number of α-type bosons' worldlines of $x(y)$ direction. The supercounterflow (paired superfluid) order is present if $\rho_{SC} > 0$ and $\rho_{SP} = 0$ ($\rho_{SP} > 0$ and $\rho_{SC} = 0$). All the kinds of stiffness vanish inside the MI region, thus confirming the absence of those SF orders. This validates the use of the effective action (2) that consists only of the order parameter of single-particle SF ψ_α. In Fig. 4, we also find $\rho_{SC} > \rho_{SP}$, i.e., $\langle W_A \cdot W_B \rangle < 0$, which is consistent with the prediction of the effective attractive interaction $u_{AB} < 0$.

Next let us consider the finite-temperature phase diagram. While the nature of the finite temperature transition differs from that at zero temperature, the transition temperature T_c near a second-order QPT is governed by the quantum criticality [44,45]. The critical behavior of T_c is of particular importance in the sense that it has been directly measured in recent experiments in both contexts of ^{4}He films [46] and optical lattices loaded with ultracold gases
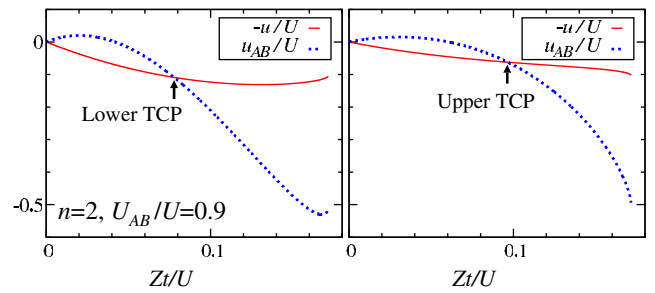
FIG. 3 (color online). Zt/U dependence of $-u/U$ and u_{AB}/U at $U_{AB}/U = 0.9$, for the lower (left panel) and upper (right panel) edges of the lobe by Ginzburg-Landau expansion of energy density from $|n_A, n_B\rangle = |1, 1\rangle$.
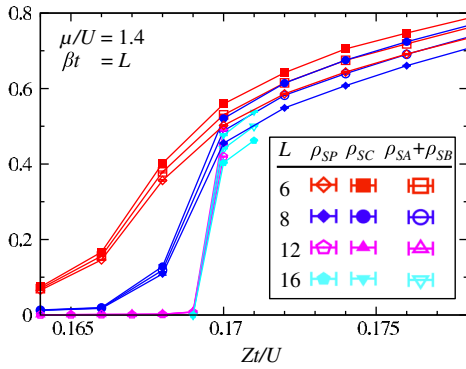
FIG. 4 (color online). The SF stiffness $\rho_{SA} + \rho_{SB}$, ρ_{SC}, and ρ_{SP} computed by QMC simulations at $\beta t = L$ and $\mu/U = 1.4$.

FIG. 5 (color online). Results of QMC simulations at finite temperature. (a) Transition temperatures at $Zt/U = 0.04$, 0.08, 0.12, and 0.16. Circles (blue) and squares (red) represent the first-order and BKT transitions, respectively. (b) Temperature dependence of ρ_{SA} at $Zt/U = 0.08$ and $\mu/U = 0.96$. (c) Chemical potential dependence of ρ_{SA} at $Zt/U = 0.16$ and $\beta t = 12$.

[13]. On the basis of the effective model (2), we derive the critical behavior of T_c that is summarized in Table I (see the Supplemental Material [41] for details). As expected, the critical behaviors for the generic QPT are the same as that for the vacuum-SF QPT of a dilute Bose gas [45,47,48], and these QPTs belong to the same universality class. In contrast, the tricritical behavior is distinctly different from the standard one; specifically, $T_c \propto \delta\mu^{1/d}$ if we disregard the logarithmic contributions in $d = 2$.

Figure 5 shows the transition temperatures as functions of μ/U obtained from QMC simulations for several values of Zt/U. The transition temperatures are estimated from jumps of ρ_{SA} and n. If a transition to the SF phase is of the Berezinskii-Kosterlitz-Thouless (BKT) type, it is well known that ρ_{SA} exhibits the universal jump $\Delta\rho_{SA} = T/(t\pi)$, at the transition point [49]. Thus the BKT transition temperature is estimated from the cross point of $T/(t\pi)$ and $\rho_{SA}(L = 48)$ as shown in Fig. 5(b). On the other hand, ρ_{SA} shows a larger jump than $T/(t\pi)$ at the first-order phase transition. As shown in Fig. 5(c), we find the first-order phase transition at finite temperatures. This means that there is a tricritical line in the $T - t - \mu$ phase diagram and the quantum TCPs are its end points.

To examine the shift of the criticality from $T_c \propto \delta\mu$ (generic) to $\propto \delta\mu^{1/2}$ (tricritical), we fit T_c/t by assuming a fitting function $T_{\text{fit}}(\delta\bar{\mu}) = [C_1^2 + C_2\delta\bar{\mu}]^{1/2} - C_1$ with fitting parameters $C_{1,2}$, where $\delta\bar{\mu} \equiv \delta\mu/U$. Since $T_{\text{fit}} \propto \delta\bar{\mu}^{1/2}$ for $C_1 = 0$ while $T_{\text{fit}} \propto \delta\bar{\mu}$ for $C_1 > 0$ at small $\delta\bar{\mu}$, the approach to the tricritical behavior can be identified as the decrease of C_1 towards zero. By the fitting to the numerical data in Fig. 5(a), we indeed find that C_1 at the TCP, i.e., $Zt/U = 0.12$, is much closer to zero compared to C_1 for the generic QPTs ($Zt/U = 0.04$ and 0.08). Thus, the tricritical behavior of T_c has been corroborated. Notice that within the temperature range of our numerical simulations the fitting function that neglects logarithmic contributions fits better to the data than the one with logarithmic contributions, as was also the case in previous experiments [13,46].

In conclusion, we have computed the ground-state and finite-temperature phase diagrams near the $n = 2$ Mott lobe of the two-component BHM in square lattices by the QMC method. It was shown that the SF-MI transition is of first order near the tip of the Mott lobe while it is of second order far from the tip. We have identified the TCPs on the SF-MI phase boundary. Since the model is a quantitative counterpart of a realistic experimental system, namely, a Bose-Bose mixture in an optical lattice, this finding of the TCPs makes it possible for optical-lattice experiments to address the issue of quantum tricriticality. Moreover, we have derived critical behaviors of the QPT across the TCP. The predicted quantum tricritical behavior of the SF-normal transition temperature may be examined in future experiments.

[1] M. Greiner, O. Mandel, T. Esslinger, T. W. Hänsch, and I. Bloch, Nature (London) **415**, 39 (2002).
[2] T. Stöferle, H. Moritz, C. Schori, M. Köhl, and T. Esslinger, Phys. Rev. Lett. **92**, 130403 (2004).
[3] I. B. Spielman, W. D. Phillips, and J. V. Porto, Phys. Rev. Lett. **98**, 080404 (2007).
[4] C. Becker, P. Soltan-Panahi, J. Kronjäger, S. Dörscher, K. Bongs, and K. Sengstock, New J. Phys. **12**, 065025 (2010).

[5] M. Pasienski, D. McKay, M. White, and B. Demarco, Nat. Phys. **6**, 677 (2010).

[6] B. Gadway, D. Pertot, J. Reeves, M. Vogt, and D. Schneble, Phys. Rev. Lett. **107**, 145306 (2011).

[7] L. Fallani, J. E. Lye, V. Guarrera, C. Fort, and M. Inguscio, Phys. Rev. Lett. **98**, 130404 (2007).

[8] B. Deissler, M. Zaccanti, G. Roati, C. DErrico, M. Fattori, M. Modugno, G. Modugno, and M. Inguscio, Nat. Phys. **6**, 354 (2010).

[9] J. Simon, W. S. Bakr, R. Ma, M. E. Tai, P. M. Preiss, and M. Greiner, Nature (London) **472**, 307 (2011).

[10] J. Struck, C. Ölschläger, R. Le Targat, P. Soltan-Panahi, A. Eckardt, M. Lewenstein, P. Windpassinger, and K. Sengstock, Science **333**, 996 (2011).

[11] J. Struck, M. Weinberg, C. Ölschläger, P. Windpassinger, J. Simonet, K. Sengstock, R. Höppner, P. Hauke, A. Eckardt, M. Lewenstein, *et al.*, Nat. Phys. **9**, 738 (2013).

[12] M. Atala, M. Aidelsburger, J. T. Barreiro, D. Abanin, T. Kitagawa, E. Demler, and I. Bloch, arXiv:1212.0572.

[13] X. Zhang, C.-L. Hung, S.-K. Tung, and C. Chin, Science **335**, 1070 (2012).

[14] P. M. Chaikin and T. C. Lubensky, *Principles of Condensed Matter Physics* (Cambridge University Press, Cambridge, England, 2000).

[15] R. J. Birgeneau, G. Shirane, M. Blume, and W. C. Koehler, Phys. Rev. Lett. **33**, 1098 (1974).

[16] R. De Bruyn Ouboter, K. W. Taconis, C. Le Pair, and J. J. M. Beenakker, Physica (Utrecht) **26**, 853 (1960).

[17] T. Misawa, Y. Yamaji, and M. Imada, J. Phys. Soc. Jpn. **78**, 084707 (2009).

[18] P. Jakubczyk, J. Bauer, and W. Metzner, Phys. Rev. B **82**, 045103 (2010).

[19] M. Stephanov, K. Rajagopal, and E. Shuryak, Phys. Rev. Lett. **81**, 4816 (1998).

[20] N. Kawashima and K. Harada, J. Phys. Soc. Jpn. **73**, 1379 (2004).

[21] M. Anderlini, P. J. Lee, B. L. Brown, J. Sebby-Strabley, W. D. Phillips, and J. V. Porto, Nature (London) **448**, 452 (2007).

[22] S. Trotzky, P. Cheinet, S. Fölling, M. Feld, U. Schnorrberger, A. M. Rey, A. Polkovnikov, E. A. Demler, M. D. Lukin, and I. Bloch, Science **319**, 295 (2008).

[23] A. Widera, S. Trotzky, P. Cheinet, S. Fölling, F. Gerbier, I. Bloch, V. Gritsev, M. D. Lukin, and E. Demler, Phys. Rev. Lett. **100**, 140401 (2008).

[24] J. Catani, L. De Sarlo, G. Barontini, F. Minardi, and M. Inguscio, Phys. Rev. A **77**, 011603 (2008).

[25] D. M. Weld, P. Medley, H. Miyake, D. Hucul, D. E. Pritchard, and W. Ketterle, Phys. Rev. Lett. **103**, 245301 (2009).

[26] B. Gadway, D. Pertot, R. Reimann, and D. Schneble, Phys. Rev. Lett. **105**, 045303 (2010).

[27] D. Jaksch, C. Bruder, J. I. Cirac, C. W. Gardiner, and P. Zoller, Phys. Rev. Lett. **81**, 3108 (1998).

[28] G. Thalhammer, G. Barontini, L. De Sarlo, J. Catani, F. Minardi, and M. Inguscio, Phys. Rev. Lett. **100**, 210402 (2008).

[29] S. Tojo, Y. Taguchi, Y. Masuyama, T. Hayashi, H. Saito, and T. Hirano, Phys. Rev. A **82**, 033609 (2010).

[30] D. McKay and B. DeMarco, New J. Phys. **12**, 055013 (2010).

[31] A. Kuklov, N. Prokofev, and B. Svistunov, Phys. Rev. Lett. **92**, 050402 (2004).

[32] T. Ozaki, I. Danshita, and T. Nikuni, arXiv:1210.1370.

[33] D. Yamamoto, T. Ozaki, C. A. R. Sá de Melo, and I. Danshita, Phys. Rev. A **88**, 033624 (2013).

[34] T. Kimura, S. Tsuchiya, and S. Kurihara, Phys. Rev. Lett. **94**, 110403 (2005).

[35] L. de Forges de Parny, F. Hébert, V. G. Rousseau, R. T. Scalettar, and G. G. Batrouni, Phys. Rev. B **84**, 064529 (2011).

[36] Y. Kato and N. Kawashima, Phys. Rev. E **79**, 021104 (2009).

[37] O. F. Syljuåsen and A. W. Sandvik, Phys. Rev. E **66**, 046701 (2002).

[38] B. Capogrosso-Sansone, N. V. Prokof'ev, and B. V. Svistunov, Phys. Rev. B **75**, 134302 (2007).

[39] We refer to the second-order QPT other than the one at the TCP as the generic transition.

[40] W. S. Bakr, J. I. Gillen, A. Peng, S. Fölling, and M. Greiner, Nature (London) **462**, 74 (2009).

[41] See Supplemental Material at http://link.aps.org/supplemental/10.1103/PhysRevLett.112.055301 for technical detailis.

[42] D. M. Ceperley, Rev. Mod. Phys. **67**, 279 (1995).

[43] Ş. Söyler, B. Capogrosso-Sansone, N. V. Prokof'ev, and B. V. Svistunov, New J. Phys. **11**, 073036 (2009).

[44] M. P. A. Fisher, P. B. Weichman, G. Grinstein, and D. S. Fisher, Phys. Rev. B **40**, 546 (1989).

[45] S. Sachdev, *Quantum Phase Transitions* (Cambridge University Press, Cambridge, England, 2011).

[46] S. Murakawa, M. Wasai, K. Akiyama, Y. Wada, Y. Tamura, R. Nomura, and Y. Okuda, Phys. Rev. Lett. **108**, 025302 (2012).

[47] D. S. Fisher and P. C. Hohenberg, Phys. Rev. B **37**, 4936 (1988).

[48] E. B. Kolomeisky and J. P. Straley, Phys. Rev. B **46**, 11749 (1992).

[49] D. R. Nelson and J. M. Kosterlitz, Phys. Rev. Lett. **39**, 1201 (1977).